

Electrical, Structural, Magnetic and Transport Properties of $Zn_2 Ba Fe_{16} O_{27}$ Doped With Cu^{2+}

D. M. Hemed, and O.M.Hemeda
Physics Department, Faculty of Science, Tanta University, Tanta, Egypt

Abstract: Series of polycrystalline samples of $Zn_{2-x}Cu_x Ba Fe_{16} O_{27}$ were prepared by usual ceramic methods, where (x=0.0, 0.4, 0.6, 0.8, 1.0, 1.4). X-ray analysis were obtained at room temperature using Cok_a with $I = 1.790A^0$ confirmed the presence of W-type hexaferrite phase structure. Saturation magnetization and hysteresis loops curves measurements at room temperature were studied as a function of Cu^{2+} substitution. It can be seen that the Cu^{2+} content slightly decreases the saturation magnetization from 25 to 20 (emu g^{-1}), all hysteresis loops are closed which indicates low anisotropy field and low saturation magnetization field. The dc conductivity and thermoelectric power was measured in range from room temperature up to $T = 750 K$ for all samples. The thermoelectric power decreases by increasing Cu^{2+} content and the conductivity increases with temperature. The value of the charge carrier concentration increases by increasing temperature and Cu^{2+} content.

Key words: Magnetic properties, Electrical properties, charge carrier concentration X-ray analysis, Hexagonal ferrite

INTRODUCTION

Hexaferrite powder with a narrow size distribution are promising materials for industrial applications due to their high coercivities and their moderate saturation magnetization^[1-4]. Polycrystalline hexaferrite are very useful for microwave applications due to its very low dielectric loss. These hexaferrite can be classified into five categories^[5]: M type which has the form $Ba Me_2 Fe_{12} O_{19}$, W type or $Ba Me_2 Fe_{16} O_{27}$, Y type or $Ba Me_2 Fe_{12} O_{22}$, X-type or $Ba_2 Me_2 Fe_{28} O_{46}$ and Z-type $Ba_2 Me_2 Fe_{24} O_{41}$, where Me represent, a divalent cations of the first transition metal group e.g. Co, Ni, Mg, Zn. M and W-type hexaferrite have been studied by S. K. Mandal et al^[6].

$Cu Fe_2 O_4$ is a collinear ferrimagnet of spinel structure showing spontaneous magnetization below $T_N = 743 K$ ^[7]. This ferrite when slowly cooled starting from high temperatures has a tetragonal deformed spinel structure below 630 – 660 K. The cubic form of $Cu Fe_2 O_4$ is obtained by heat treatment, that is quenching at high temperature^[8]. The crystallographic phases differ in their magnetization and magneto

crystalline anisotropy^[9]. Then copper ferrite is commonly known to appear in two structural form: a cubic one of spinel type (space group $\Gamma d3m$) and a tetragonal one of space group I_4 ^[10]. The tetragonal is due to the Jahn-Teller effect of Cu^{2+} ions located at octahedral B sites^[11]. A temperature of 650 K corresponds to the crystal distortion from tetragonal to cubic form was observed^[12] in $Cu Fe_2 O_4$. The neel temperature T_N was determined to be 756 K. So we can say that copper ferrite is distinguished among other spinel ferrite by the fact that it undergoes a structural phase transition at 650 K accompanied by a reduction in crystal symmetry to tetragonal due to the cooperative Jahn-Teller effect^[13]. Magnetic and crystallographic studies on copper ferrite^[14] have revealed that this ferrites have a formula: $(Cu_d Fe_{1-d})^A [Cu_{1-d} Fe_{1+d}]^B O_4$ where d is an inversion parameter. The tetragonal to cubic transformation depends upon the ratio of Cu ions at tetrahedral and octahedral sites of the spinel lattice, which in turns depends on the thermal history of the sample.

Corresponding Author: D. M. Hemed, and O.M.Hemeda, Physics Department, Faculty of Science, Tanta University, Tanta, Egypt

RESULTS AND DISCUSSION

1- X- Ray diffraction of $Zn_{2-x}Cu_xBaFe_{16}O_{27}$: The x-ray diffraction patterns of the samples $Zn_{2-x}Cu_xBaFe_{16}O_{27}$ where ($x = 0.0, 0.4, 0.6, 0.8, 1.0,$ and 1.4) were obtained at room temperature using Cok_{α} with $\lambda = 1.7902 \text{ \AA}$ (this study was conducted in faculty of science Tanta University) . Fig. (1.a,b) shows the x-ray diffraction pattern for the above mentioned compositions . The diffraction patterns confirm the presence of W- type hexaferrite phase structure. The lattice parameters were calculated from the relation [13].

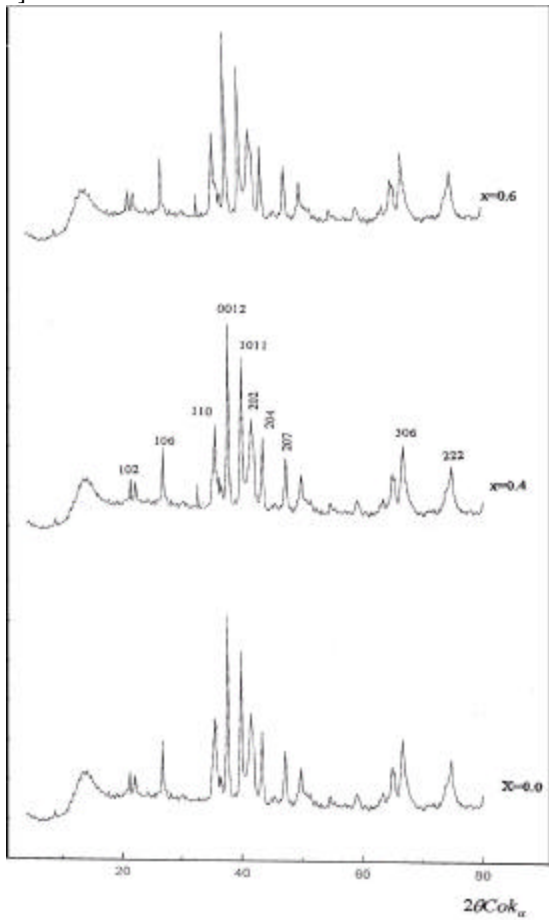
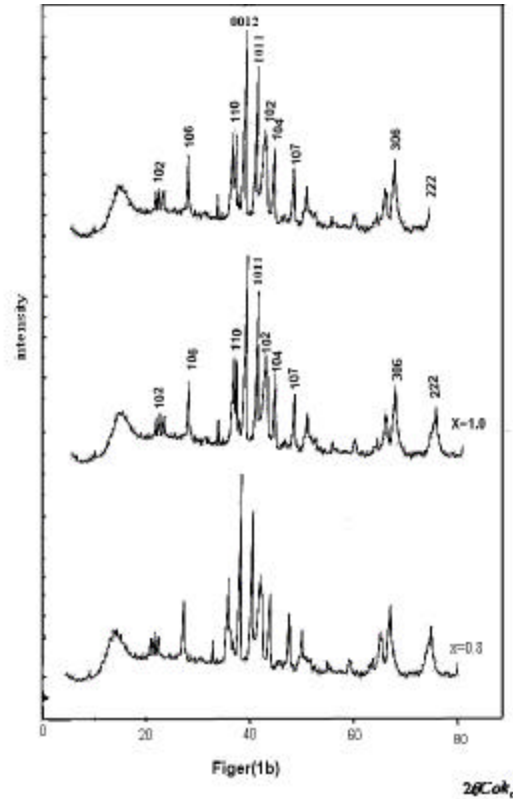


Figure (1a)

Fig. 1a: X-ray diffraction pattern of $Zn_{2-x}Cu_xBaFe_{16}O_{27}$ hexagonal ferrite at room temperature ($x=0.0, 0.4, 0.6$)



x-ray diffraction pattern for the samples ($x=0.8, 1.0, 1.4$) which indicates tetragonal phase
($2\theta=21.78, 32.72, 36.3, 39.43$ and 41.75)

Fig. 1b: X-ray diffraction pattern for the samples ($x=0.8, 1.0, 1.4$)

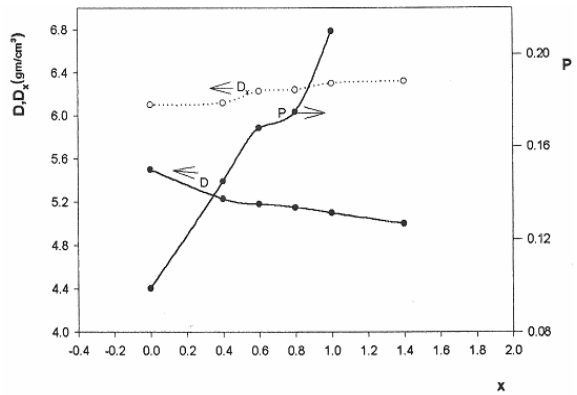


Figure (2)

Fig. 2: The bulk density, X-Ray density and porosity as a function of Cu additions

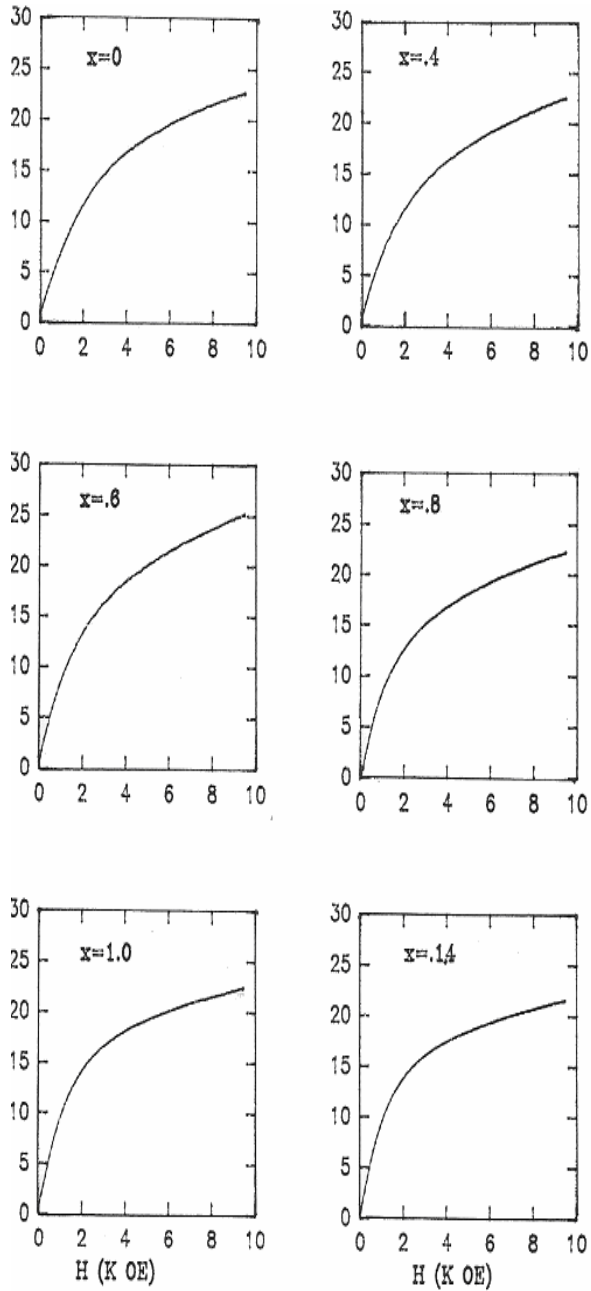


Figure (3)

Fig.3: The initial magnetization curves

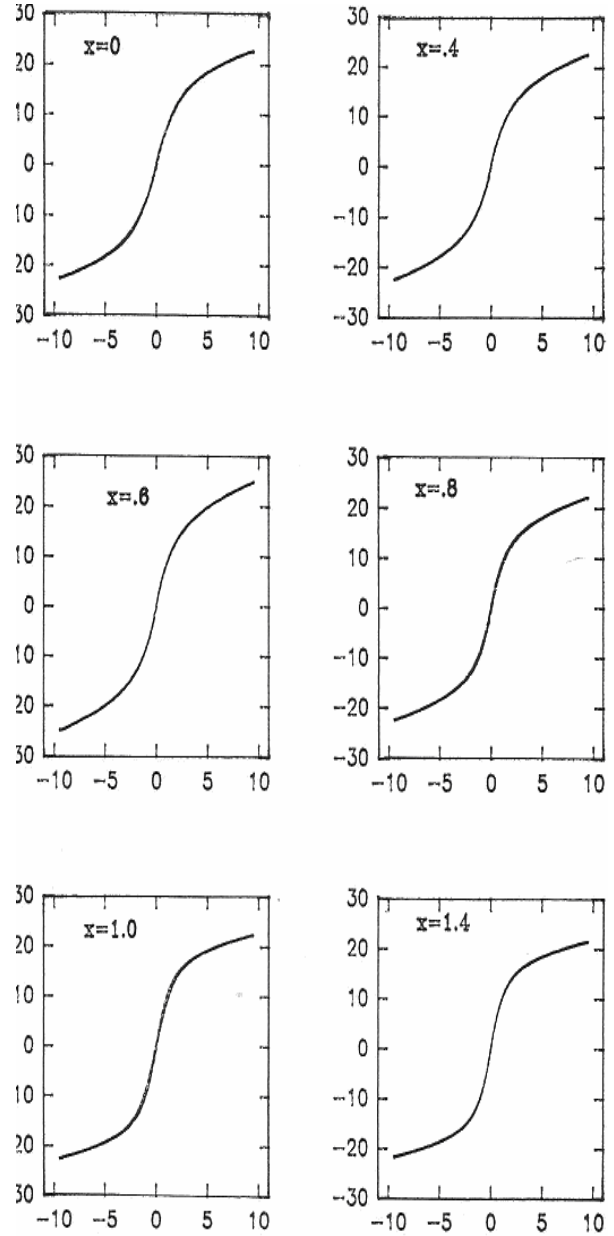


Figure (4)

Fig. 4: the magnetic hesteresis loops

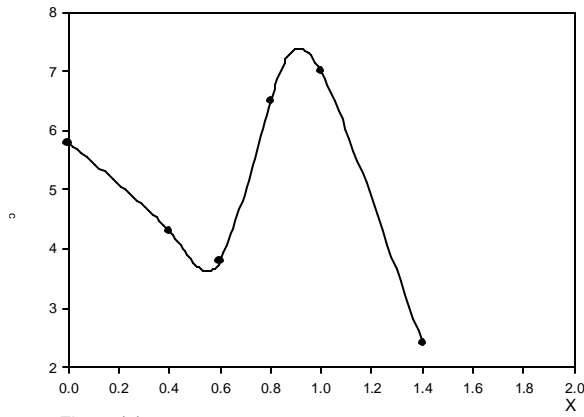


Figure (5)

Fig. 5: The coercivity as a function of Cu additions

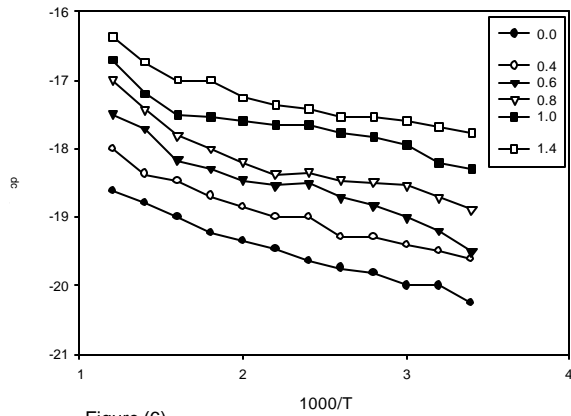


Figure (6)

Fig.6: DC conductivity as a function of (1000/ T)

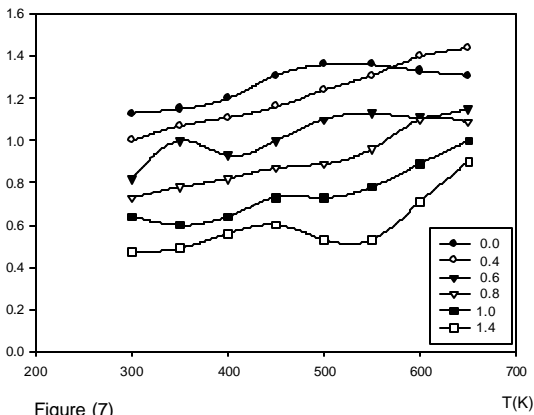
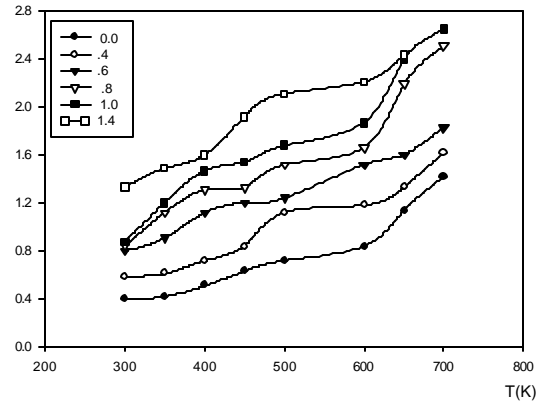


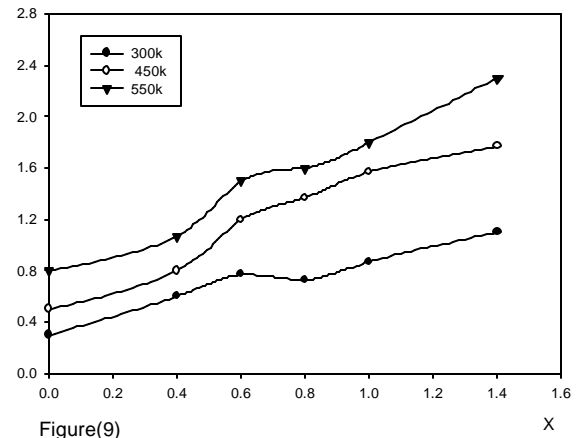
Figure (7)

Fig. 7: Seebeck coefficient as a function of absolute temperature



Figure(8)

Fig. 8: Concentration of charge carriers as a function of temperatures



Figure(9)

Fig. 9: Concentration of charge carriers as a function Cu additions

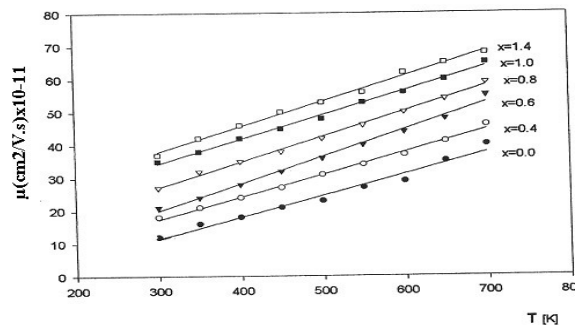


Figure (10)

Fig. 10: Charge carriers mobility as a function of absolute temperature

$$\frac{1}{d^2_{hkl}} = \frac{4}{3} \frac{b^2 + hk + k^2}{a^2} + \frac{l^2}{c^2} \quad (1)$$

Where d_{hkl} is the interplanar distance. The variation of lattice parameter a , c and their ratio c/a versus Cu substitution are given in table (1). It is shown that c , a and their ratio c/a are nearly constant with increasing Cu content. This behavior can be explained on the basis of ionic radii of substituted ions where, the ionic radius of Cu^{2+} ions is 0.072 nm which is nearly of the same order of that of Zn^{2+} ions (0.074 nm). This confirms that Cu^{2+} ion replace Zn^{2+} ion in the structure. The value of the lattice parameters for our structure are $a = 5.85$ nm and $c = 33.7$ nm. The X-ray diffraction patterns indicates the presence of tetragonal phase due to the Jahn-Teller effect produced by Cu^{2+} ions located at octahedral B sites. There are some peaks appear in the patterns of the sample contains Cu^{2+} ion and belongs to tetragonal phase. These peaks appeared at $2\theta = 21.75, 32.72, 36.3, 39.43$ and 41.75 with corresponding d values equals $4.74, 3.18, 2.87, 2.62$ and 2.51 nm.

For the hexagonal structure, the x ray density is calculated according to the relation

$$D_x = \frac{2M}{NV} \quad (2)$$

Where V is the volume of the unit cell $V = a^2 c \sin 120^\circ$, M is the molecular weight and N is Avogadro's number. The porosity P was calculated for each sample from the relation:

$$P = 1 - \frac{D}{D_x} \quad (3)$$

The experimental density D and the porosity P , were calculated for each composition.

Fig (2) shows the variation of the experimental density D , X-ray density D_x and the porosity P , as a function of copper content (x). It is shown that the experimental density is slightly decreases with increase of Cu content but the porosity is slightly increases. This behavior may be attributed to the facts that the introduction of Cu ions in hexagonal ferrite may affect the grain size development during sintering and increase the porosity. The X-ray density was calculated from XRD data and was found nearly equal to 6.102 gm/cm³ which is higher than the bulk density. We can conclude that the Cu addition retards the sintering process and decreases the grain size leading to the increase of the porosity.

Magnetic Study: The magnetic properties of $\text{Zn}_{2-x}\text{Cu}_x\text{BaFe}_{16}\text{O}_{27}$ have been investigated by saturation magnetization M_s curves and hysteresis curves measurements at room temperature. It can be seen that the Cu^{2+} substitution slightly decreases the saturation magnetization from 25 (at $x = 0.6$) to 20 (at $x = 0.4$) (emu g⁻¹) as shown in Fig. (3). The substitution of Cu^{2+} at octahedral sites instead of Zn^{2+} replaces some Fe^{3+} ions from B to A sites, which decreases the net magnetic moment of the sample and so decrease M_s . The substitution of Cu^{2+} ions is a mechanism that gives rise to spin canting phenomena which decrease the saturation magnetization [14]. Very recently, Morales et al. [15] proposed that the spin canting may originate from cationic vacancies disorder. In the given ferrite, the substitution of Cu^{2+} instead of Zn^{2+} produce vacancies. These vacancies originates spin canting which reduces the M_s due to cationic redistribution during substitution [16]. From the hysteresis loop Fig. (4) it can be seen that all loops are closed which indicates low anisotropy field and low saturation magnetization field.

The copper ferrite is known to be magnetically soft, with value of coercivity of about 0.7 kOe at room temperature for bulk material [17]. For hexagonal Cu ferrite, these values are different as shown in Fig. (5). It is known that Cu^{2+} substitution shows a marked Jahn-Teller effect arising from the doubling degenerate type ground state of the Cu^{2+} ions [18]. The local distortion gives rise to fluctuation of the spin exchange interaction and so changes the magnetic properties. The full saturation is not reached at 5 kOe for samples suggesting a spin canting structure forming during substitution process. The oxygen vacancies produced by substitution process break the $\text{Fe}-\text{O}-\text{Fe}$ superexchange path. As known, the A-B interaction are stronger than A-A or B-B interaction. Additionally in Cu ferrite, the $\text{Fe}^{3+}-\text{O}-\text{Cu}^{2+}$ superexchange interaction are weaker than the corresponding $\text{Fe}^{3+}-\text{O}-\text{Fe}^{2+}$ [19]. Therefore, the redistribution of Cu^{2+} and Fe^{3+} ions between A and B sites can effectively modify the super exchange interaction and lowering the local field of the given Fe^{3+} sites and decreases the M_s .

The variation of M_s can be explained on the basis of cation distribution and exchange interaction. The substitution of Zn by Cu at octahedral sites weakened the strength of A-B interaction as suggested by Yafet and Kittel [20]. The increase in Cu content increases the triangular spin arrangement at B-sites, tending to a reduction of A-B interaction

and the decreasing of M_s . From micro structural analysis, our results shows the increase of the porosity with the increase of Cu, this is in good agreement with results reported earlier for mixed ferrite^[20]. The variation in the coercivity H_c with Cu addition can be correlated fairly with the Neel's mechanical model treating the demagnetizing influence of nonmagnetic material^[21]. The decrease of H_c at higher Cu content with the increasing of porosity, means that a less demagnetizing field is required to vanish the magnetization, due to the presence of pores.

Electrical and transport properties: Fig. 6 illustrates the variation of the dc conductivity and thermoelectric coefficient (α) with temperature for all samples in the range from room temperature up to $T=750K$. It can be seen that the temperature increases, the $\ln S_{dc}$, increases linearly, according to the

$$\text{Arrhenius equation: } S_{dc} = S_0 \exp \frac{-E}{k_B T} \quad (4)$$

where E is the activation energy for conduction, S_0 is the pre-exponential constant, k_B is Boltzmann's constant, and T is solute temperature. The conductivity S_{dc} Vs temperature have three regions with two breaks. The first break at lower temperature is due to the structural phase transition from tetrahedral to cubic structure. The second break at higher temperature (T_c) assigned to the magnetic order phase transition from ferri to paramagnetic state. It is noticed that the Curie temperature T_c of the given ferrite shifts to lower temperature and the point corresponds to the structural phase transition shifts to higher temperature which make it more stable at high Cu content.

These results are in agreement with previous work^[12,13]. The two crystallographic phases are different in their magnetic properties especially in magnetization and crystalline anisotropy. At this temperature small abrupt rises in S is formed.

This transition is first order phase transition^[22]. The structural phase transition occurs at a temperature below curie temperature, due to the cooperative Jahn-Teller effect. Fig.(7) indicates the relation between thermoelectric power (α) and temperature. The general behavior of (α) indicates that the majority carriers are electron due to the electron hopping between $Fe^{3+} \xrightarrow{e} Fe^{2+}$. The thermoelectric coefficient

(α) decreases by increasing Cu content due to the hopping holes between $Cu^{2+} \xleftarrow{h} Cu^{1+}$. The seeback coefficient for all samples is slightly increases by increasing temperature from 300 – 750 K as in Fig. (7) which means that the dominant conduction process is hopping conduction and the minority conduction process is due to impurities. The charge carriers concentration (n) as calculated for the region at which α is constant using the relation^[23]

$$\alpha = \frac{-2.3k_B}{e} \log \left(\frac{N}{n} - 1 \right) \quad (5)$$

where N is the density of state or concentration level involved in the conduction process, n is the charge carrier concentration and k_B is Boltzmann's constant.

The value of N can be taken as 10^{22} ion/cm^3 ^[24]. The value of n (Concentration of charge carriers) as a function of temperature and Cu addition are shown in Fig. (8), Fig. (9) respectively. Fig. 7,8 show that the relation between α, n vs T have three regions, and two breaks correspond to the structural phase transition and the magnetic order phase transition. The values of n and α for magnetic region show that the conductivity increases due to thermally activation of charge carrier mobility and not due to the increase of n . This is the cause of hopping mechanism.

The dc electrical conductivity can be written as sum of two terms:

$$S_{dc} = e(n_e m_e + n_p m_p) \quad (6)$$

where n_e and n_p are the concentration of negative and positive charge carriers, m_e

and m_p are their mobility respectively. By using the experimental values of electrical conductivities and the values of charge carriers concentration n , the charge carrier mobility m was calculated at different temperature and different Cu content from the relation $\mu=1/ne$. The charge carrier mobility is shown in Fig. (10) as a function of temperature and Cu content. It is observed that charge carrier mobility increases by increasing temperature and Cu content. The drift mobility is thermally activated and gives a breaks at temperatures near the same value given from the conductivity versus temperature. The increase of electrical conductivity in this case is mainly due to the increase of drift mobility and not due to the increase of

charge carrier's concentration.

CONCLUSION

The decrease of H_c with the increasing of porosity, means a less demagnetizing field is required and will result in decrease in saturation magnetization until the demagnetizing field is equal to the coercive force. The increase in Cu content increases the triangular spin arrangement at B – sites, tending to a reduction of A – B interaction and the decreasing of M_s . The variation in the coercive force with Cu addition can be correlated fairly with the Neel's mechanical model treating the demagnetizing influence of nonmagnetic material. The increase of electrical conductivity is mainly due to the increase of drift mobility and not to the increase of charge carrier's concentration.

The charge carrier concentration still nearly constant at ferromagnetic region by increasing temperature. The result of electrical conductivity and thermoelectric power show that the material has hopping conduction at ferromagnetic region.

The general behavior of (α) indicates that the majority carriers are electron due to the electron hopping between $Fe^{3+} \xleftarrow{e} Fe^{2+}$. The thermoelectric coefficient (α) decreases by increasing Cu content due to the hopping holes between $Cu^{2+} \xleftarrow{h} Cu^{1+}$.

REFERENCE

1. R. H. Vidora, 1988. J. Appl. Phys. 63: 3423
2. Atare, I. R. Harris, C. B., 1995. Ponton, J. Mater. Sci. 30:1429
3. F. Wat, J. Rivas, D. Martinez and H. Kronmuller, 1994, Phys. Stat. Sol. (a) 143:137
4. T. O. Kuzmitchera, L.P. Ophovik and V. P. Shabatin, 1995 IEEE, Tras. Mag. 31:800
5. M. El-Saadawy, 1999. Materials Letters 39:149 – 197
6. S. K. Mandal, K. Singh and D. Bahadur, 1994. J. Mater. Sci 29:3738
7. H. Ohnishi and T. Jeranishi, 1961. J. Phys. Soc. Japan 16:35
8. T. Miyadai, Si Miyahara and Y. Matsuo, 1965. J. phys. Soc. Japan 20: 980
9. H. Nagata, T. Miyadai and. Miyahara, 1972. IEEE Trans. Magnetics 8 : 451
10. E. Prince and R. G. . 1956 Treuting, Acta cryst. 9: 1025
11. R. L. White and D. A. Herman, 1973. proc. Internat. Conf. Magnetism, Vo13, Moscow: 64
12. I. Onyszkiewicz, Thesis, 1980. A. Mickiewicz University, poznon
13. I. Onyszkiewicz, N. T. Malafaev, A. A. Murakhovskii, J. A. Popko, 1990. Journal of Magnetism and Magnetic materials, 89:8
14. I. Onyszkiewicz, Acta physica polonica, 1985. Vol. A 68 447
15. M. P. Morales, C. J. Serna, F. Badker and S. Marup, 1954. J. Phys. Condens. Matter 9
16. J. Z. iang, G. F. Goya and H. R. Rechenberg, 1999 J. Phys. Condens. Matter 11: 4063
17. Goya G. F. H. R. Rechenberg and J. Z. Jiang, 1998. J. Appl. Phys. 84 1101
18. G. F. Goya and H. R. 1998, rechenberg, nanostructured materials, Vol. 10, No. 6, 1001
19. G. F. Goya and H. R. Rechenberg, 1998. J. Phys. Condens. Matter 10:11829
20. J. Eckelt, ch . Bottger and J. hesse, 1992. J. Mag. Mag. Mater 104:1665
21. M. th. Rekvedlt, 1989. Texture and microstructure, 11:127
22. J. Kubiak and J. Pietrzak, 1981. Phys. Stat. Sal. (a) 67:103
23. J. B. Goodenoagh 1970, Mater. Res. Bull: 621
24. R. R. Heiks and W. D. Johnston, J. Chem. 1957 Phys. 26:582